Structural plasticity and catalysis regulation of a thermosensor histidine kinase

Daniela Albanesi[a,b,1], Mariana Martín[b,1], Felipe Trajtenberg[c], María C. Mansilla[b], Ahmed Haouz[d], Pedro M. Alzari[a], Diego de Mendoza[b], and Alejandro Buschiazzo[a,c,2]

[a]Institut Pasteur, Unité de Biochimie Structurale and [d]Plateforme de Cristallogenèse et Diffraction de Rayons X, URA 2185 Centre National de la Recherche Scientifique, Paris 75015, France; [b]Instituto de Biología Molecular y Celular de Rosario, Departamento de Microbiología, Facultad de Ciencias Bioquímicas y Farmacéuticas, Universidad Nacional de Rosario, Rosario 2000, Argentina; and [c]Institut Pasteur de Montevideo, Unidad de Cristalografía de Proteínas, Montevideo 11400, Uruguay

Edited by E. Peter Greenberg, University of Washington School of Medicine, Seattle, WA, and approved August 3, 2009 (received for review June 15, 2009)

Temperature sensing is essential for the survival of living cells. A major challenge is to understand how a biological thermometer processes thermal information to optimize cellular functions. Using structural and biochemical approaches, we show that the thermosensitive histidine kinase, DesK, from *Bacillus subtilis* is cold-activated through specific interhelical rearrangements in its central four-helix bundle domain. As revealed by the crystal structures of DesK in different functional states, the plasticity of this helical domain influences the catalytic activities of the protein, either by modifying the mobility of the ATP-binding domains for autokinase activity or by modulating binding of the cognate response regulator to sustain the phosphotransferase and phosphatase activities. The structural and biochemical data suggest a model in which the transmembrane sensor domain of DesK promotes these structural changes through conformational signals transmitted by the membrane-connecting two-helical coiled-coil, ultimately controlling the alternation between output autokinase and phosphatase activities. The structural comparison of the different DesK variants indicates that incoming signals can take the form of helix rotations and asymmetric helical bends similar to those reported for other sensing systems, suggesting that a similar switching mechanism could be operational in a wide range of sensor histidine kinases.

coiled-coil | conformational rearrangement | crystallography | signal transduction

Cold sensors are ubiquitous integral membrane proteins found in all kingdoms of life. They are involved in many physiological roles, including membrane remodeling, chemotaxis, touch, and pain (1–3). The histidine kinase (HK), DesK, from *Bacillus subtilis* is the founding example of a membrane-bound thermosensor suited to remodel membrane fluidity when the ambient temperature drops below approximately 30 °C (Fig. S1). Several lines of evidence show that the cold thermal stimulus is detected by DesK, which together with the response regulator (RR), DesR, constitutes a canonical two-component system (TCS). In vivo experiments have demonstrated that DesK acts as a kinase at cold temperatures (4), ultimately activating the transcription of the gene *des* coding for the acyl lipid desaturase Δ5-Des (1, 5). The increased fraction of unsaturated fatty acids in the membrane then restores fluidity and shuts off the kinase activity of DesK, terminating transcription.

Histidine kinases are multifunctional enzymes that share a conserved intracellular catalytic core linked to a high diversity of signal-sensing domains. Through still poorly understood mechanisms, HKs are able to catalyze autokinase, phosphotransferase, and protein phosphatase reactions in response to external stimuli, ultimately controlling the degree of phosphorylation of their cognate RR and hence the functional outcome of the signaling pathway. DesK is a class I HK (6) with an N-terminal sensor domain (≈150 residues) composed of four or five transmembrane (TM) segments connected to a C-terminal cytoplasmic domain (DesKC, ≈220 residues) (4) that belongs to the HisKA_3 subfamily (PFAM 00730) of HKs (7). To investigate how fluctuations in ambient temperature regulate the catalytic activities of DesK, we solved the crystal structure of its catalytic core in different functional states and determined the functional properties of the full-length sensor in pure lipids vesicles. The results highlight the remarkable plasticity of the central four-helix bundle domain as the protein proceeds along the catalytic cycle, and suggest a signal-dependent regulation model that may be operational in a wide range of HKs.

Results

To uncover the structural features of DesK associated with the different functional states of the protein, we carried out structural studies of DesKC before and after autophosphorylation. We also characterized two point mutants of the catalytic domain, in which the phosphorylatable histidine residue (H188) was substituted either by valine ($DesKC_{H188V}$), a mutant known to retain the phosphatase activity of the wild-type protein (4), or by glutamic acid ($DesKC_{H188E}$), sought to mimic the phosphorylated state of the enzyme. The 3D structures of the different DesKC variants were determined in six different crystalline environments (Table 1) using multiwavelength anomalous diffraction (MAD) and molecular replacement methods (*SI Text* and Table S1).

The catalytic core of DesK (Fig. 1 *A*–*C*) shows the characteristic homodimeric structure observed in other HKs (8). Each monomer consists of an N-terminal antiparallel 2-helix hairpin (helices α1 and α2) that includes the phoshorylatable H188, connected by a short linker region (residues 243–245) to a C-terminal ATP-binding domain (ABD). The helical hairpins of two monomers interact with each other to form a central four-helix bundle (4-HB) domain, known as the DHp (for Dimerization and Histidine phosphotransfer) domain. In each monomer, the N-terminal part of helix α1 extends beyond the 4-HB, connecting the catalytic core with the TM sensor domain. The structure of the ABD, composed by a five-stranded β-sheet opposed by a layer of three α-helices, is similar to that of other members of the GHKL superfamily (9) and remains essentially unchanged in the different DesKC structures (Fig. 1*D*), except for a high mobility of the ATP lid.

Three Distinct Conformational States of DesKC Variants. The structures of DesKC reveal three distinct conformational states of the

Author contributions: A.H., P.M.A., D.d.M., and A.B. designed research; D.A., M.M., F.T., A.H., P.M.A., D.d.M., and A.B. performed research; D.A., M.M., F.T., M.C.M., and A.H. contributed new reagents/analytic tools; D.A., M.M., F.T., M.C.M., P.M.A., D.d.M., and A.B. analyzed data; and P.M.A., D.d.M., and A.B. wrote the paper.

The authors declare no conflict of interest.

This article is a PNAS Direct Submission.

Freely available online through the PNAS open access option.

Data deposition: The atomic coordinates and structure factors have been deposited in the Protein Data Bank, www.pdb.org (PDB ID codes 3EHF, 3EHH, 3EHJ, 3GIE, 3GIF, and 3GIG).

[1]D.A. and M.M. contributed equally to this work.

[2]To whom correspondence should be addressed. E-mail: alebus@pasteur.edu.uy.

This article contains supporting information online at www.pnas.org/cgi/content/full/0906699106/DCSupplemental.

Table 1. Crystal structures of DesKC variants

Structure	DesKC modification	Ligand	Resolution, Å
$DesKC_{\Delta 174}$	Short construct*	AMP-PCP	3.1
DesKC-P	Phosphorylated	AMP-PCP	3.5
E188a	His188-Glu	ADP	2.7
E188b	His188-Glu	AMP-PCP	2.65
V188a	His188-Val	AMP-PCP	2.5
V188b	His188-Val	ADP	2.1

Further details are provided in Table S1.
*The DesKC construct includes only the catalytic core (residues 175–370).

protein, differing in the interhelical packing of the central DHp domain and the relative mobility and orientation of the ABDs. As indicated by the overall root-mean-square deviations (rmsd) between all identical residues of the homodimer (Table S2), two conformational states can be assigned respectively to unphosphorylated (Fig. 1*A*) and phosphorylated (Fig. 1*B*) DesKC (respectively, $DesKC_{\Delta 174}$ and DesKC-P, rmsd of 12.7 Å). The third conformational state is represented by two independent structures of the mutant $DesKC_{H188V}$ (monoclinic V188a and orthorhombic V188b) (Fig. 1*C*), which are similar to each other (rmsd of 1.13 Å) but significantly different from the previous structures (rmsd values of 14.2–15.9 Å). Finally, the independent structures of the point mutant $DesKC_{H188E}$ (orthorhombic E188a and monoclinic E188b) are respectively closer to those of phosphorylated DesKC (rmsd of 2.2 Å between E188a and DesKC-P, Fig. 1*B*) and unphosphorylated DesKC (rmsd of 3.77 Å between E188b and $DesKC_{\Delta 174}$, Fig. 1*A*) than to each other (rmsd of 9.5 Å between E188a and E188b). The higher rmsd between $DesKC_{\Delta 174}$ and E188b is not due to the modified side chain, which is fully solvated and not involved in intramolecular interactions, but to the internal flexibility of the protein (Fig. S2), stabilized by a different molecular environment in each case. Although the DesKC homodimer exhibits rather extensive intermolecular contacts in some crystal forms, these interactions appear to have only a marginal effect on the observed conformational states, because the same overall structure has been obtained in two distinct crystal forms for each state.

$DesKC_{\Delta 174}$ and E188b Display Mobile ATP-Binding Domains. The DHp domain in $DesKC_{\Delta 174}$ and E188b is a left-handed antiparallel coiled-coil (10) similar to other dimerization domains of the HK superfamily. The core of the 4-HB is stabilized by eight layers of hydrophobic residues, corresponding to four coiled-coil heptad repeats (11) on helices α1 and α2. The heptad positions can be identified with letters from *a* to *g* (12), where *a* and *d* are the expected hydrophobic residues involved in the interface. The key interacting positions (shown in Fig. 1*E*) involve mostly hydrophobic aminoacids, which are conserved in a large majority of HKs belonging to the HisKA_3 subfamily. Assignment of these residues to alternate *a* and *d* positions (Fig. 1*E*) requires a single residue insertion ('skip' residue) just after L187 '*a*', an insertion that promotes formation of a helical bulge at the phosphorylatable H188 to preserve the hydrophobic core (Fig. S3*A*). Interestingly, a helical kink in the same region is promoted in other HKs by the presence of a highly conserved proline (absent in DesK), as seen in the structures of TM0853 (13) and KinB (14), the only other two HKs for which the structure of the entire cytoplasmic domain is available.

The conformational state typified by the structures of $DesKC_{\Delta 174}$ and E188b (Fig. 1*A*) is characterized by a flexible quaternary organization. The individual ABDs in each structure are either not visible in the electron density (as in $DesKC_{\Delta 174}$, which lacks the 20 N-terminal residues of helix α1) or show few, non-specific interactions with this region, outside the 4-HB (as in E188b, which includes the entire cytoplasmic domain). This internal flexibility contrasts with the more extensive DHp-ABD association observed in both TM0853 and KinB, and is suggestive of an autokinase-competent

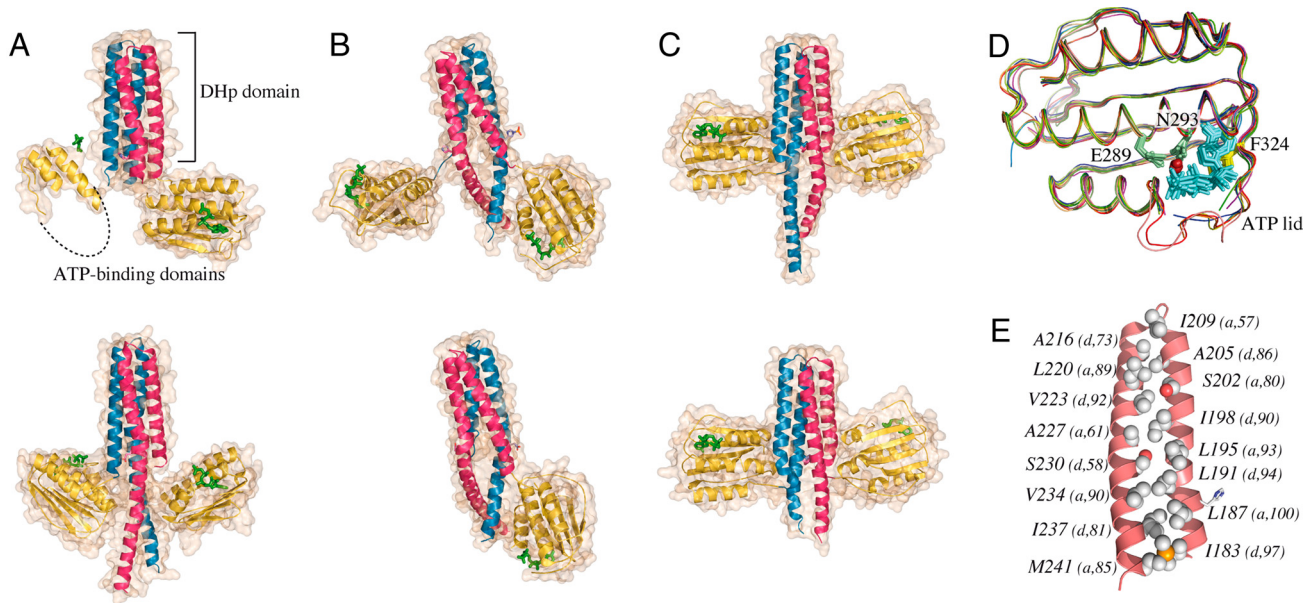

Fig. 1. Three distinct conformational states of DesKC. Cartoon representations of the DesK homodimers, with the two α-helical hairpins from the DHp domain highlighted in pink (α1) and blue (α2), the ABDs colored in yellow, and bound nucleotides in green. (*A*) Overall structures of $DesKC_{\Delta 174}$ (*Top*) and E188b (*Bottom*), with mobile ABDs. (*B*) Structure of DesKC-P (*Top*), similar to E188a (*Bottom*), rotated approximately 60° around the vertical axis with respect to (*A*) for clarity. (*C*) Structures of V188a (*Top*) and V188b (*Bottom*). (*D*) Superposition of the 11 independent ABDs seen in all DesKC variants. The bound nucleotide is shown in cyan, with the adenine ring stacked against F324 (in yellow). The Mg^{2+} ion (in red) contacts the nucleotide phosphates and two residues (E289 and N293, in green) that belong to the conserved N box (17). The ATP-lid (residues 321–334) shows the largest structural differences and is partially disordered in many crystal structures. (*E*) Hydrophobic residues (CPK spheres) of one helical hairpin that, upon dimerization, forms the core of the 4-HB in $DesKC_{\Delta 174}$. For each residue, its *a/d* position within the heptad repeats and the percentage of members of the HisKA_3 subfamily having a hydrophobic residue (AVLMI) at the same position are indicated in parenthesis.

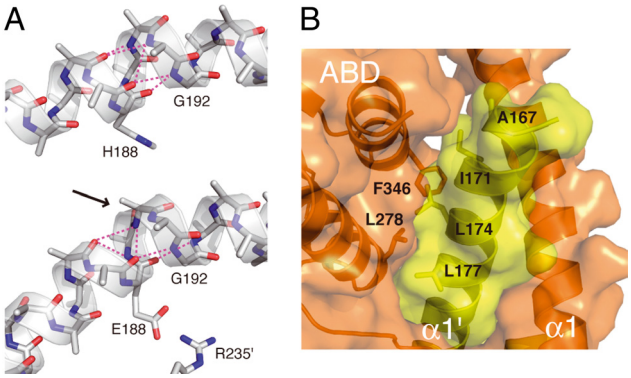

Fig. 2. Pronounced helical bending in phosphorylated DesKC. (*A*) The pattern of intrahelical H bonds in monomer A of DesKC-P (*Top*) and E188a (*Bottom*) around the phosphorylatable histidine is modified as a consequence of a helical bulge, facilitated by the presence of a conserved glycine (G192). Note that the carbonyl oxygen of D189 (arrow) is not involved in H bond interactions. Other side-chains are omitted for clarity. (*B*) Close view of the interaction between helix α1 and the ABD from the opposite monomer in E188a.

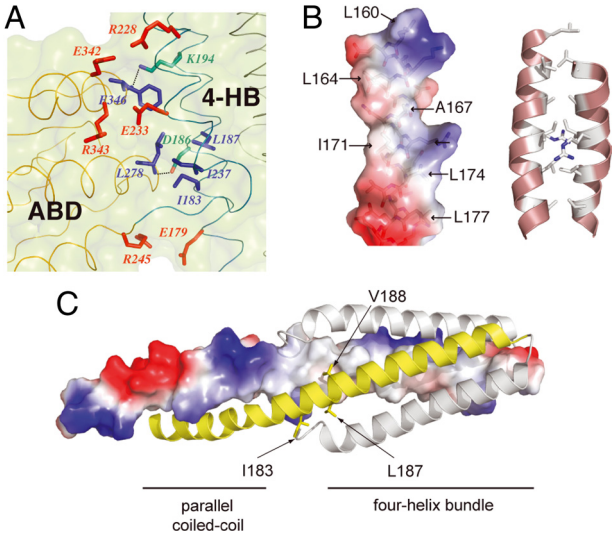

Fig. 3. Extensive intradomain interactions in DesKC$_{H188V}$. (*A*) Close view of the interaction between the ABDs and the DHp domain in DesKC$_{H188V}$. Key residues are colored according to the type of interaction (electrostatic in red, hydrophobic in blue, and H-bonding in green). (*B*) Cartoon representation (*Right*) of the two-helical coiled-coil formed by the homodimerization of residues 160–180. Core hydrophobic residues are shown in stick representation. Molecular surface representation (*Left*) of the same helical region for one monomer, showing the exposed hydrophobic patch. (*C*) Overall view of the parallel coiled-coil and the 4-HB in DesKC$_{H188V}$. The molecular surface color-coded according to electrostatic charges is shown for helix α1 in one monomer. The side-chains of I183 and L187, which were part of the DHp core in DesKC$_{Δ174}$, are now at the outer surface of the domain (engaged in interactions with the ABD domain, not shown).

(K$^+$) state. Indeed, a single rigid-body rotation movement pivoting on the interdomain hinge residue G243 can bring the nucleotide γ-phosphate from one ABD into physical contact with the fully exposed imidazole ring of H188 in the second protomer. The contact surfaces display a good overall complementarity (Fig. S4) and several conserved residues are favorably positioned to mediate DHp-ABD domain interactions, including two predicted salt bridges (K296-D189 and R235-E289), the presence of a glycine at position 192 providing space to accommodate the γ-phosphate *en transfer*, and an exposed patch of basic residues on the DHp that is well located to interact with acidic residues in the ATP-lid of the ABD (Fig. S4*B*). This model is consistent with *trans* autophosphorylation within the homodimer (15), because intramonomeric phosphorylation would require the partial, but energetically costly, unwinding of the DHp α2 helix in the absence of a longer, flexible linker (16). Experimental evidence among members of this and other subfamilies, will ultimately lead to a full understanding of autophosphorylation mechanisms, not excluding HK clusters displaying *cis*-phosphorylation in the case of significantly different interdomain organization.

DesKC-P and E188a Exhibit an Asymmetric Homodimer with a Pronounced Helical Bending. To obtain structural information on the phosphotransferase-competent state of DesKC, we not only used the DesKC$_{H188E}$ mutant, but also exploited the alkaline stability of the phosphoramidate bond by carrying out the autophosphorylation reaction at pH 8.5 before crystallogenesis. The 3D structures of DesKC-P and the orthorhombic form of DesKC$_{H188E}$ (E188a) reveal a similar asymmetric homodimer (Fig. 1*B*), in which one ABD interacts with the central helix α1 while the other is either disordered (E188a) or makes no contacts with the rest of the protein (DesKC-P). A pronounced bending angle of helix α1 is seen in both monomers, with values in the range 33–35° and 50–54° for each of them. The phosphorylation-induced change in helical direction promotes a local rearrangement of intrahelical hydrogen bonds at the kink position near H188 (Fig. 2*A*), possibly facilitated by a higher mobility of this region as seen for EnvZ (17). As mentioned before, the same kink is also present in unphosphorylated DesKC (Fig. S3*B*), but in this case the bending angle of helix α1 is much smaller (12–19° for all independent monomers in DesKC$_{Δ174}$ and E188b).

The asymmetric conformation and pronounced helical bending appear to be stabilized by two different factors: the partial association between the ABD and the central helical domain and the electrostatic interaction of the phosphohistidine (or the E188 carboxylate) with conserved basic residues. The ABD association involves a hydrophobic contact surface of 420–450 Å^2 between two regions of the ABD (the N terminus of α4 and the C terminus of α5) and a patch of hydrophobic residues on one face of helix α1′ (including A167′, I171′, L174′ and L177′) from the opposite monomer (Fig. 2*B*). Steric clashes in helix α1 preclude a similar interaction to occur simultaneously in both monomers, accounting in part for the observed conformational asymmetry. In DesKC-P the electron density maps strongly suggest the presence of a phosphate group attached to one H188 residue within the dimer, although the low resolution of this structure prevents a detailed analysis. Instead, in the analogous E188a structure the carboxylate group of E188 from each monomer forms a salt-bridge with either R235 or K242 from the opposite protomer (Fig. S3*C*), two positions at which a basic residue is conserved in a large majority of members of the HisKA_3 subfamily. These observations strongly argue for the functional relevance of the asymmetric DesKC conformation, in agreement with recent reports emphasizing the importance of structural asymmetry in other signal transduction systems (18, 19).

The Mutation H188V Triggers Formation of an N-terminal 2-Helical Coiled-Coil and Extensive DHp-ABD Association. The substitution of H188 by valine provides a suitable model for the phosphatase-competent state of DesK, because DesKC$_{H188V}$ was shown to retain specific phosphatase activity toward the response regulator DesR at comparable levels to those of wild-type DesK, both in vitro and in vivo (4). The two independent structures of DesKC$_{H188V}$ are very similar, showing a more compact and rigid conformation (Fig. 1*C*) than those of the previous DesKC variants. This is due to extensive intramolecular interactions involving both a tighter DHp-ABD interaction in each monomer and the formation of a parallel 2-helix coiled-coil, which continues the 4-HB toward the membrane in full-length DesK. The DHp-ABD association (Fig. 3*A*) is comparable to that observed in the two other HKs of known structure,

TM0853 and KinB (13, 14). The interaction buries approximately 1,100–1,200 Å^2 and includes hydrophobic contacts (I183, L187, and I237 from the DHp and L278 and F346 from the ABD), two H-bonds (K194NZ-F346O and D186OD2-L278N and three salt bridges (E179-R245; E233-R343; and E342-R228). The interacting surface on the DHp domain was first identified as a weakly conserved motif in HKs (20) and mutations mapping in this region were found in EnvZ when searching for mutants that abrogated phosphatase activity (21), suggesting the importance of ABD sequestering for this reaction.

The coiled-coil structure of the 4-HB in DesKC$_{H188V}$ continues toward the N terminus through a parallel left-handed 2-helix coiled-coil at the N-terminal region (Fig. 3*B*), a feature not seen in the other structures. This 2-helix coiled-coil increases the dimerization interface of the protein (≈1,800 Å^2 compared to ≈1,450 Å^2 in the 4-HB alone) and includes three heptad repeats, with the internal hydrophobic positions occupied by L160 (*d*), L164 (*a*), A167 (*d*), I171 (*a*), L174 (*d*), and L177 (*g*) (Fig. 3*B*). The connection of these heptad repeats with those of the 4-HB (Fig. 1*D*) implies a 'stutter' (12) or deletion of three positions between L177 and Q181. Formation of the 2-helical coiled-coil has two important consequences. First, they relieve the bulge on helical turn 187–191 observed in the previous structures, now showing a regular α-helical architecture and a 'diamond'-shaped cross-section of the bundle (Fig. S5*A*). Second, a hydrophobic patch (including I183 and L187) in helix α1, which was buried within the DHp core in both DesKC$_{Δ174}$ and DesKC-P (Fig. 1*D*), is now accessible at the DHp surface for interaction with the ABD (Fig. 3*C*).

Although the overall structural change is triggered by the point mutation (as the valine side chain is buried in the interhelical core of V188a/b), the structures support the functional relevance of DesKC$_{H188V}$ as a bona fide representative of the phosphatase-active state of DesK. The fairly extensive DHp-ABD and monomer-monomer interfaces (totaling ≈3,000 Å^2 in the homodimer) that stabilize the observed conformation strongly argue for its physiological relevance. In wild-type DesK, a similar conformation (partially burying H188) might be achieved through the structural constraints imposed by the TM domain. Furthermore, the helical rearrangement in DesKC$_{H188V}$ is similar to that of TM0853, allowing formation of the membrane-connecting 2-helix coiled-coil as a left-handed extension of the 4-HB (Fig. 3*C*). Finally, it was convincingly shown for TM0853 that ABD sequestration by the DHp domain regulates kinase activity (13), suggesting that the comparable DHp-ABD interaction in DesKC$_{H188V}$ might fulfill a similar role.

Temperature Regulation of DesK Catalytic Activities. To investigate the link between the conformational states described above and catalysis regulation, it is crucial to elucidate how the cold signal modulates the different enzymatic activities of DesK. Our previous genetic studies have shown that DesK can assume different signaling states in response to membrane fluidity (22). To provide a solid biochemical ground to these observations, we studied the influence of temperature on the catalytic activities of DesK in a functional in vitro reconstituted system. Full-length DesK was expressed in a cell-free system and co-translationally integrated into liposomes of *E. coli* phospholipids (23). These lipids undergo a reversible change of state from a fluid (disordered) to a non-fluid (ordered) array of fatty acyl chains when the temperature is decreased from 37 °C to 25 °C (24).

As shown in Fig. 4*A* (*Left*), the autokinase activity of DesK was significantly up-regulated (≈50-fold) when temperature was decreased. Truncation of the TM segments resulted in a constitutive K^+ state (Fig. 4*A*, *Right*) demonstrating that the TM domain of DesK stabilizes a kinase-repressed state at higher temperatures. On the other hand, DesK-stimulated dephosphorylation of phospho-DesR was significantly lower at 25 °C than at 37 °C (Fig. 4*B*, *Left*). This thermal response also required the TM domain (Fig. 4*B*, *Right*), ruling out a simple temperature effect on enzyme activity. In contrast, we were unable to detect temperature-induced changes in the initial rates of phosphotransferase activity, which result in phosphoryl migration from DesK to DesR (Fig. 4*C*). After longer incubation times the levels of phosphorylated DesR were lower at high temperature, probably due to the up-regulated phosphatase activity of DesK. Taken together, the above experiments clearly demonstrate that (1) the temperature stimuli come directly from the membrane lipid bilayer, with no other proteins involved in the sensing or signaling mechanisms, (2) the cold signal regulates the autokinase and phosphatase activities of DesK in opposite directions, and (3) the TM domain plays a crucial sensing and regulatory role, because the cytoplasmic domain alone (DesKC) is unresponsive to the cold signal.

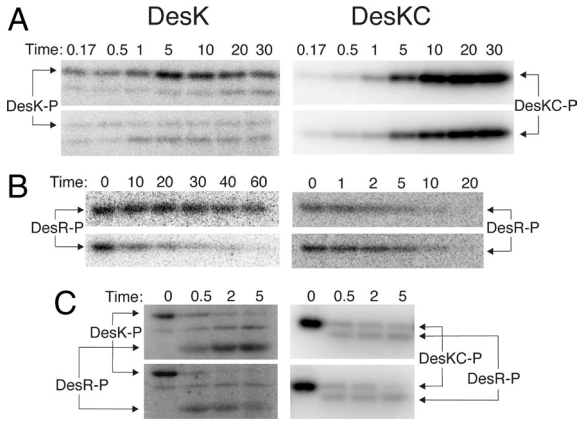

Fig. 4. Biochemical characterization of DesK proteoliposomes. Left (DesK inserted in liposomes) and right (soluble DesKC) panels show (*A*) autokinase, (*B*) phosphatase, and (*C*) phosphotransferase activities at the indicated times (min), assayed at 25 °C (*Top*) and 37 °C (*Bottom*). To perform DesK phosphotransferase activity assays, the protein was first allowed to autophosphorylate at 25 °C and subsequently incubated with DesR at both temperatures. The bands corresponding to each phosphorylated protein are indicated, see *SI Text* and Fig. S7 for further details.

Interhelical Rearrangements in the DHp Domain Modulate Intradomain and Protein-Protein Interactions. The crystallographic studies of DesK highlight the structural plasticity of the central DHp domain and suggest an important role of these changes in catalysis regulation. Thus, formation of the parallel two-helix coiled-coil concomitantly generates the DHp interface to bind the ABD, shutting off autokinase activity. The observed DHp rearrangements also modify the molecular surface around the phosphorylatable H188 (Fig. S5*B*), poised to interact with DesR (in phosphotransfer or phosphatase interactions) or with the mobile ABD (during autophosphorylation catalysis). Consistently, both DesKC$_{H188V}$ and DesKC$_{H188E}$ were found to produce a stable Mg^{2+}-dependent complex with DesR, separable by size exclusion chromatography (Fig. S6 *A* and *B*), as expected if the DesKC-P/E188a and V188a/b structures do represent the phosphotransferase and phosphatase-competent states of DesKC, respectively. In contrast, no stable association of DesR with DesKC could be detected under the same experimental conditions (Fig. S6*C*). This interaction could only be rescued after adding ATP, suggesting that DesKC phosphorylation triggers a conformational transition (confirmed also by SEC, Fig. S6*D*), from the autokinase to a phosphotransferase-competent state.

Comparison of the V188a/b structures with those in other conformational states reveals a composite movement in the DHp domain, combining a rotational shift through a concerted 'cog-wheel' mechanism and a shearing movement that increases the tilt angle between the two helical hairpins in the homodimer (Fig. 5*A*).

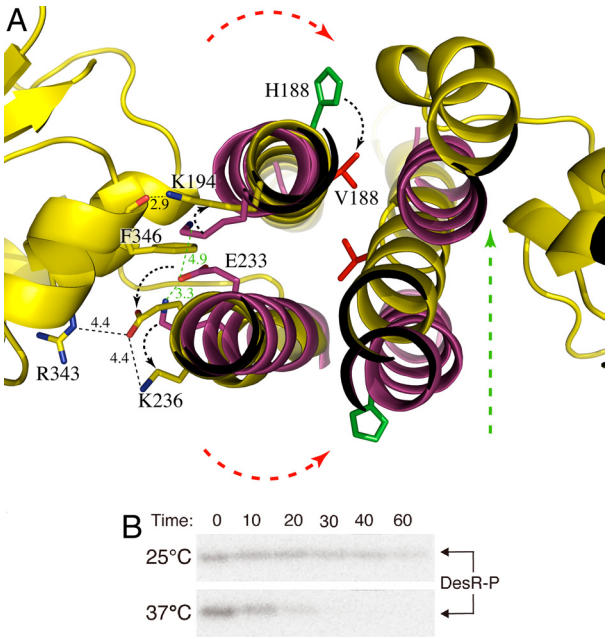

Fig. 5. Interhelical rearrangements in the DHp domain modulate intradomain and protein-protein interactions. (*A*) Cartoon representation of the helical rotations taking place in the 4-HB. The DHp helices from one monomer of $DesKC_{H188V}$ (carbon atoms in yellow) and $DesKC_{\Delta 174}$ (C atoms in magenta) are superimposed. Key residues in interdomain contacts are labeled and selected bond distances marked. Black dotted arrows connect the same residue on both structures, red dotted arrows highlight the cogwheel rotation and the green dotted arrows indicate the tilt of the two-helix hairpin. (*B*) Phosphatase activity of $DesK_{DHp}$ proteoliposomes assayed at 25 °C and 37 °C (see *SI Text* for details).

The rotational shift involves a clockwise rotation of approximately 60° around the helix axis of α1 residues 175–189 and a comparable counterclockwise rotation of α2 residues 233–241. Such a 'cogwheel' rotation, required to generate or disrupt both the membrane-connecting two-helix coiled-coil and the ABD-interacting site in $DesKC_{H188V}$ (Fig. 5*A*), is fully consistent with conformational signals propagated across helical coiled-coils involved in signal transduction (25).

A crucial issue to validate our structural interpretation is to assess whether the observed interhelical rotational rearrangements do occur in solution during the catalytic cycle. Since the introduction of point mutations or external probes to monitor these changes might directly modify the 4-HB structure, we used a functional approach based on a deletion mutant missing the ABDs. The rationale behind this approach is that the DHp domain alone retains a measurable phosphatase activity (21). Thus, a deletion mutant of DesK including the TM and the DHp domains but not the ABD ($DesK_{DHp}$, residues 1–242) was produced and its phosphatase activity assayed in proteoliposomes at different temperatures. As shown in Fig. 5*B*, this construct displayed a temperature-regulated phosphatase profile comparable to that of full-length DesK (Fig. 4*B*), clearly indicating that propagation of the cold signal from the membrane triggers a conformational change in the DHp domain itself.

Discussion

The conformational flexibility of α-helical coiled-coils is a well-documented phenomenon (26, 27), allowing for functionally relevant conformational heterogeneity and low interconversion energy barriers among alternate configurations. Our structural data of DesKC now provide strong evidence that the DHp domain is marginally stable and prone to rotational rearrangements in the context of the full-length protein. Furthermore, these structural changes have a direct effect on the functional properties of DesK, since modifications of the DHp molecular surface were shown to modulate both interdomain interactions (DHp-ABD) as well as protein-protein association (DesK-DesR) required for catalysis.

The crystal structures of DesKC reveal three distinct conformational states of the protein (Fig. 1 *A–C* and Table S2), characterized by a highly dynamic nature of the ABDs. This flexibility (particularly in $DesKC_{\Delta 174}$, DesKC-P, and the phospho-mimic $DesKC_{H188E}$) hampers crystallization and might explain why these states have not been previously observed in other HKs. While the actual nature of the DesK signaling intermediates remains to be elucidated, our structural and biochemical data indicate that the observed conformations of DesKC exhibit distinctive properties that can be respectively associated with the kinase-competent ($DesKC_{\Delta 174}$, E188b), phosphotransferase-competent (DesKC-P, E188a), and phosphatase-competent (V188a, V188b) states of the protein.

Based on these structural results and the observation that the temperature signal regulates the autokinase and phosphatase activities of DesK in opposite directions (Fig. 4), we can propose a simple regulation model for DesK (Fig. 6). In a fluid membrane, the TM domain would stabilize the connecting coiled-coil and the catalytic core into a more compact conformation, as seen for $DesKC_{H188V}$, with the ABDs attached to the DHp domain (Fig. 6, *Left*). This conformation inhibits autokinase activity and the DHp surface is competent to interact with DesR (Fig. S6*A*), resulting in

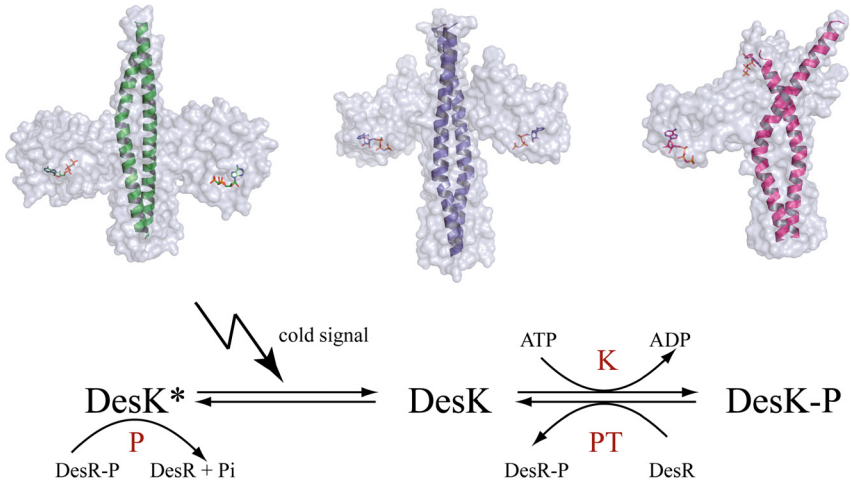

Fig. 6. Proposed model of catalysis regulation. The observed structures of the DesKC homodimer (shown as surface models with helix α1 highlighted) are ascribed to the three functional states of the kinase: phosphatase-competent (DesK*), kinase-competent (DesK), and phosphotransferase-competent (DesK-P). The corresponding reactions (P, K, PT) are indicated in the lower panel.

a (K^-/P^+) phenotype. Upon cold signal reception, the ensuing structural reorganization would release the ABDs for histidine phosphorylation, as seen in $DesKC_{\Delta 174}$ (Fig. 6, *Center*). Compelling mutagenesis evidence supporting the importance of weakening the DHp-ABD association for autokinase activity has been previously obtained for TM0853 (13). In this functional state, two distinct factors contribute to down-regulate DesK phosphatase activity. First, the modified DHp interaction surface precludes DesK/DesR binding, as suggested by the lack of complex formation of the unphosphorylated proteins (Fig. S6*C*). Second, the dynamic effect of the released ABDs, covalently attached to the DHp domain, could also contribute to decrease the resultant DesR-binding affinity due to a higher effective concentration. These mechanisms (surface modulation, ABD mobility) are not mutually exclusive and are amenable to fine-tuning in different HKs. Phosphorylation of DesKC induces an as yet different, asymmetric conformation with a pronounced bending of helix $\alpha 1$ (Fig. 6, *Right*), capable of interacting with DesR (Fig. S6*B*). Crystallization of $DesKC_{H188E}$ in two distinct conformations, respectively similar to $DesKC_{\Delta 174}$ (autokinase) and DesKC-P (phosphotransferase), suggest a low interconversion energy barrier between these functional states. As a consequence, the corresponding structural transition could be induced, in the absence of external stimuli, by phosphate attachment to or transfer from H188 (as proposed in Fig. 6, *Lower*).

The proposed model of catalysis regulation in DesK, governed by interhelical rearrangements in the DHp coiled-coil, may be a common trait for a large fraction of HKs. Alpha helices are indeed common information transducer elements (28) and different types of helical movements performing mechanical work have been proposed to convey input/output signals (29–31). Furthermore, incoming signals in the form of helix rotations are congruent with mechanistic models derived from the study of upstream elements in different signal transducing systems. Thus, the parallel coiled-coil HAMP domain, present in the membrane-connecting region of several HKs (32), was shown to relay the input signal through helical rotations (25) compatible with the structural changes seen in DesK. Also, a combined helical rotation and tilting was involved in signal transduction by the bacterial sensory rhodopsin phototactic receptor (33) and analogous rotational movements were recently proposed as a general mechanism of signal transduction through α-helical coiled-coil linkers (34).

Materials and Methods

Protein Production and Crystallization. All recombinant proteins were produced and purified as described in *SI Text*. For DesKC phosphorylation, the protein (10 mg/mL) was preincubated in 50 mM Tris-HCl, pH 8.5, with 5 mM ATP and 10 mM $MgCl_2$ for 1 h at room temperature. All proteins were preincubated with 5 mM AMP-PCP or ADP (as indicated for each structure in Table S1) before crystallization. Initial crystallogenesis screenings were performed as described in *SI Text*. After optimization, crystals were grown at 18 °C by mixing 2 mL protein solution (10 mg/mL) and 2 mL reservoir solution in hanging drops. Reservoir solutions contained: 10% PEG-3350, 0.1 M Bicine, pH 9, 0.1 M $CaCl_2$, and 30% glycerol (V188a, V188b); 18% PEG-8000, 0.1 M Mes, pH 6.5, and 0.2 M calcium acetate ($DesKC_{\Delta 174}$); 10% PEG 3000, 0.1 M CHES, pH 9.5, and 10 mM $MgCl_2$ (DesKC-P, 7 mg/mL); 14% MPD, 0.1 M HEPES, pH 6, and 10 mM $MgCl_2$ (E188b); and 14% PEG-3350, 0.1 M Tris, pH 7, 5 mM KCl, and 50 mM $CaCl_2$ (E188a).

Crystallographic Studies. Single crystals were cryoprotected in mother liquor containing 25% glycerol (or 22% MPD) and flash frozen in liquid N_2 before X-ray data collection; all diffraction data sets were processed according to standard procedures (full details in *SI Text* and Table S1). The structures were solved by multiwavelength anomalous diffraction (MAD), using SeMet-labeled proteins, except for DesKC-P and $DesKC_{H188E}$, which were solved by molecular replacement methods. Complete procedures of data processing, selenium substructure determination and protein phasing/refinement are detailed in *SI Text*; final refinement parameters are given in Table S1.

Size-Exclusion Chromatography. Proteins (1–1.5 mg/mL) were preincubated with 10 mM $MgCl_2$ and 5 mM ADP or ATP for 30 min and then injected in a Superdex75 10/300 column (GE Healthcare), equilibrated in 50 mM HEPES, pH 7.5, 0.3 M NaCl, and 10 mM $MgCl_2$ and run at 0.5 mL/min.

Proteoliposomes Obtainment, Purification, and Activity Characterization. The synthesis and purification of DesK proteoliposomes and the enzyme activity assays were performed following the published method (23), with the modifications described in *SI Text*.

ACKNOWLEDGMENTS. We thank the staff of the Unidad de Bioquímica Analítica (Inst Pasteur Montevideo) for mass spectrometry analyses and of beamlines ID23-1, ID14-4 and ID-29 (European Synchrotron Radiation Facility) for diffraction data collection. This work was supported by grants from Agencia Nacional de Investigación e Innovación, Uruguay; Agence Nationale de la Recherche, France; Institut Pasteur (France); Consejo Nacional de Investigaciones Científicas y Técnicas, Argentina; Agencia de Promoción Científica y Tecnológica, Argentina; and ECOS France-Argentine Action Grant A05B02. D.A. is a Marie Curie Incoming International Fellow (European Union), F.T. is a fellow from Agencia Nacional de Investigación e Innovación, and D.d.M. is an International Research Scholar from the Howard Hughes Medical Institute.

1. Aguilar PS, Hernandez-Arriaga AM, Cybulski LE, Erazo AC, de Mendoza D (2001) Molecular basis of thermosensing: A two-component signal transduction thermometer in Bacillus subtilis. *EMBO J* 20:1681–1691.
2. Dhaka A, et al. (2007) TRPM8 is required for cold sensation in mice. *Neuron* 54:371–378.
3. Salman H, Libchaber A (2007) A concentration-dependent switch in the bacterial response to temperature. *Nat Cell Biol* 9:1098–1100.
4. Albanesi D, Mansilla MC, de Mendoza D (2004) The membrane fluidity sensor DesK of *Bacillus subtilis* controls the signal decay of its cognate response regulator. *J Bacteriol* 186:2655–2663.
5. Cybulski LE, del Solar G, Craig PO, Espinosa M, de Mendoza D (2004) *Bacillus subtilis* DesR functions as a phosphorylation-activated switch to control membrane lipid fluidity. *J Biol Chem* 279:39340–39347.
6. Bilwes AM, Alex LA, Crane BR, Simon MI (1999) Structure of CheA, a signal-transducing histidine kinase. *Cell* 96:131–141.
7. Finn RD, et al. (2008) The Pfam protein families database. *Nucleic Acids Res* 36:D281–288.
8. Varughese KI, Madhusudan, Zhou XZ, Whiteley JM, Hoch JA (1998) Formation of a novel four-helix bundle and molecular recognition sites by dimerization of a response regulator phosphotransferase. *Mol Cell* 2:485–493.
9. Dutta R, Inouye M (2000) GHKL, an emergent ATPase/kinase superfamily. *Trends Biochem Sci* 25:24–28.
10. Walshaw J, Woolfson DN (2001) Open-and-shut cases in coiled-coil assembly: Alpha-sheets and alpha-cylinders. *Protein Sci* 10:668–673.
11. Crick F (1953) The packing of alpha-helices: Simple coiled-coils. *Acta Crystallogr* 6:689–697.
12. Lupas AN, Gruber M (2005) The structure of alpha-helical coiled coils. *Adv Protein Chem* 70:37–78.
13. Marina A, Waldburger CD, Hendrickson WA (2005) Structure of the entire cytoplasmic portion of a sensor histidine-kinase protein. *EMBO J* 24:4247–4259.
14. Bick MJ, et al. (2009) How to switch off a histidine kinase: Crystal structure of *Geobacillus stearothermophilus* KinB with the inhibitor Sda. *J Mol Biol* 386:163–177.
15. Cai SJ, Inouye M (2003) Spontaneous subunit exchange and biochemical evidence for trans-autophosphorylation in a dimer of *Escherichia coli* histidine kinase (EnvZ). *J Mol Biol* 329:495–503.
16. Park H, Saha SK, Inouye M (1998) Two-domain reconstitution of a functional protein histidine kinase. *Proc Natl Acad Sci USA* 95:6728–6732.
17. Tanaka T, et al. (1998) NMR structure of the histidine kinase domain of the *E. coli* osmosensor EnvZ. *Nature* 396:88–92.
18. Neiditch MB, et al. (2006) Ligand-induced asymmetry in histidine sensor kinase complex regulates quorum sensing. *Cell* 126:1095–1108.
19. Pollard AM, Bilwes AM, Crane BR (2009) The structure of a soluble chemoreceptor suggests a mechanism for propagating conformational signals. *Biochemistry* 48:1936–1944.
20. Hsing W, Russo FD, Bernd KK, Silhavy TJ (1998) Mutations that alter the kinase and phosphatase activities of the two-component sensor EnvZ. *J Bacteriol* 180:4538–4546.
21. Zhu Y, Qin L, Yoshida T, Inouye M (2000) Phosphatase activity of histidine kinase EnvZ without kinase catalytic domain. *Proc Natl Acad Sci USA* 97:7808–7813.
22. Cybulski LE, et al. (2002) Mechanism of membrane fluidity optimization: Isothermal control of the Bacillus subtilis acyl-lipid desaturase. *Mol Microbiol* 45:1379–1388.
23. Martin M, Albanesi D, Alzari PM, de Mendoza D (2009) Functional in vitro assembly of the integral membrane bacterial thermosensor DesK. *Protein Expr Purif* 66:39–45.
24. Cronan JE, Jr, Gelmann EP (1975) Physical properties of membrane lipids: Biological relevance and regulation. *Bacteriol Rev* 39:232–256.
25. Hulko M, et al. (2006) The HAMP domain structure implies helix rotation in transmembrane signaling. *Cell* 126:929–940.
26. Deng Y, et al. (2006) Antiparallel four-stranded coiled coil specified by a 3–3-1 hydrophobic heptad repeat. *Structure* 14:247–255.
27. Yadav MK, et al. (2006) Coiled coils at the edge of configurational heterogeneity. Structural analyses of parallel and antiparallel homotetrameric coiled coils reveal configurational sensitivity to a single solvent-exposed amino acid substitution. *Biochemistry* 45:4463–4473.
28. Strickland D, Moffat K, Sosnick TR (2008) Light-activated DNA binding in a designed allosteric protein. *Proc Natl Acad Sci USA* 105:10709–10714.
29. Gao R, Lynn DG (2007) Integration of rotation and piston motions in coiled-coil signal transduction. *J Bacteriol* 189:6048–6056.
30. Kwon O, Georgellis D, Lin EC (2003) Rotational on-off switching of a hybrid membrane sensor kinase Tar-ArcB in *Escherichia coli*. *J Biol Chem* 278:13192–13195.
31. Ottemann KM, Xiao W, Shin YK, Koshland DE, Jr (1999) A piston model for transmembrane signaling of the aspartate receptor. *Science* 285:1751–1754.
32. Szurmant H, White RA, Hoch JA (2007) Sensor complexes regulating two-component signal transduction. *Curr Opin Struct Biol* 17:706–715.
33. Moukhametzianov R, et al. (2006) Development of the signal in sensory rhodopsin and its transfer to the cognate transducer. *Nature* 440:115–119.
34. Moglich A, Ayers RA, Moffat K (2009) Design and signaling mechanism of light-regulated histidine kinases. *J Mol Biol* 385:1433–1444.